CHEMICAL ENGINEERING TRANSACTIONS
VOL. 90, 2022
A publication of AIDIC
The Italian Association of Chemical Engineering
Online at www.cetjournal.it
Guest Editors: Aleš Bernatík, Bruno Fabiano

**ISBN** 978-88-95608-88-4; **ISSN** 2283-9216
DOI: 10.3303/CET2290060

# Numerical Simulation of LNG Dispersion in Harbours: a Comparison of Flammable and Visible Cloud

Mattia Carboni[a], Gianmaria Pio[b], Chiara Vianello[a,c], Paolo Mocellin[a], Giuseppe Maschio[a], Ernesto Salzano[b,*]

[a] Dipartimento di Ingegneria Industriale, Università degli Studi di Padova. Via Marzolo 9, 35131 Padova, Italia.
[b] Dipartimento di Ingegneria Civile, Chimica, Ambientale Materiali, Università di Bologna. Via Terracini 28, Bologna, Italia.
[c] Dipartimento di Ingegneria Civile, Edile e Ambientale, Università degli Studi di Padova. Via Marzolo 9, Padova, Italia
ernesto.salzano@unibo.it

The current trends in environmental impact reduction have promoted natural gas and hydrogen either as short- or long-term solutions. In both cases, liquid transportation in cryogenic form is associated with new concerns in terms of safety aspects. So far, infrastructures based on utilizing the liquefied natural gas (LNG) in port areas have been developed and realized worldwide. However, a uniform guideline and set of monitoring criteria are missing because of the lack of knowledge of the phenomenological aspects. This work deals with the numerical characterization of the visible cloud boundaries in the case of an unintentional release during bunkering operations and its comparison with the standard value for the flammability of cloud, based on the lower flammability limit. To this aim, real-scale computational fluid dynamics (CFD) simulations were performed. Results showed that both flammable and visible clouds were dramatically sensitive to the heat transfer with the substrate in an unconfined environment. Besides, turbulence seems to affect the flammable cloud expansion rather than the visible cloud. Eventually, results indicate that the flammable cloud can be up to 50% larger than the visible for confined and 20% large for unconfined environments, conservatively, on the safe side. These values can be adopted for design and emergency purposes.

## 1. Introduction

The last decades have been characterized by an exponential increase in the number of projects related to cryogenic conditions for fuel transportation because of the attractiveness of liquified natural gas (LNG) from an economic, environmental, and logistic point of view (Osorio-Tejada et al., 2017). However, significant accidents may involve seaborne cargoes and seaports (Fy et al., 2016). To reduce the impact of such events, the correct evaluation of safety distance is crucial (Chang et al., 2019). Concerning port areas, the most relevant purpose for the safe design of LNG infrastructure is the estimation of the safety distances for bunkering operations, which is typically the most hazardous operation. In this regard, the ISO 20519: 2017 (ISO 20519, 2017) and ISO/TS 18683: 2015 (ISO/TS 18683, 2015) regulate the definition of these distances and indicate the calculation procedures and allowed activities. To determine the safety zone boundaries, the ISO 20519: 2017 standard suggests the calculation of the lower flammability limit (LFL) for the LNG release under the maximum credible scenario and the rupture of the bunkering line, and it reports a simplified graph for the evaluation of the distance to LFL. In this regard, the European Maritime Safety Agency (EMSA) (EMSA, 2017) states that the ISO 20519: 2017 deterministic approach may produce impracticable safety zones and suggests the use of computational fluid dynamic (CFD) codes for more robust and reliable results. This suggestion complies with the conclusions reported by Plasmans et al. (2013), indicating CFD as a more appropriate tool than simplified models for dispersion scenarios. In this regard, it is fundamental to select an LNG evaporation rate value, the boundary conditions, and the dispersion models (Fiates et al., 2016) correctly. Regardless of the conditions, methane is an invisible substance. However, the local variation in the temperature due to the cryogenic release leads to the condensation of humidity in the atmosphere. This phenomenon forms a visible white cloud characterized by a length in a downwind direction (VISx). A dispersion safety factor (DSF) can be conveniently defined to represent

Paper Received: 22 January 2022; Revised: 7 March 2022; Accepted: 9 May 2022
Please cite this article as: Carboni M., Pio G., Vianello C., Mocellin P., Maschio G., Salzano E., 2022, Numerical simulation of LNG dispersion in harbours: a comparison of flammable and visible cloud, Chemical Engineering Transactions, 90, 355-360 DOI:10.3303/CET2290060

the ratio between the lengths of the flammable region (LFLx) to VISx. DSF can assume values either smaller or larger than unity for LNG, and it is mainly affected by the relative humidity of the atmosphere (Vilchez et al., 2013). Therefore, the effect of boundary conditions on visual identification of the cloud extinction is of interest. Recently, Agueda and co-authors have indicated a moderate but not negligible combined effect of wind speed and relative humidity on DSF (Agueda et al., 2020). Remarkably, the relative humidity of 50% has provided LFLx equal to VISx (Blackmore et al., 1982). For these reasons, this work was devoted to the numerical characterization of cloud dispersion after the accidental release of LNG at different initial conditions in terms of LFLx and VISx.

## 2. Methodology

The present study was performed using the CFD software developed by the National Institute for Standards and Technology (NIST), Fire Dynamics Simulator (FDS). This software is particularly indicated for problems involving fluids under thermal gradients and can generate combustion and soot production phenomenon (McGrattan et al., 2019a). Besides, it has already been validated for LNG consequence analysis (McGrattan et al., 2019b). In this work, the LES approach was employed for the analysis of turbulent flows. When large areas are considered, the grid is not fine enough to capture the mixing processes at all relevant scales. To this aim, a subgrid-scale model is employed (Smagorinsky, 1963). A detailed description of the database, hypothesis, and models adopted in this work can be found in the proper manual (McGrattan et al., 2019a). For the LNG case, numerical estimations have been compared with large-scale experimental campaigns, i.e., Burro, Coyote, Falcon, Maplin Sands (McGrattan et al., 2019b), reported in detail by Luketa-Hanlin (Luketa-Hanlin, 2006). In all tests, the defined physical domain is 200 m long (x-direction), 5 m height (y-direction), and 100 m wide (z-direction). A structured grid with cubic cells has been used (Pio et al., 2019). The maximum distance in the downwind direction where methane mole fraction equals the LFL (Rauchegger et al., 2015) is defined as $LFL_x$. For the scope of this work, a base case scenario was defined at first and reported in Table 1. To this aim, a total arm length of 15 m and a constant diameter of 0.30 m were considered representative for LNG bunkering and unloading operations (Nigata Loading system LTD, 2019). Assuming that the inventory of the outboard arm (i.e., the descending part) forms the pool, the released volume of LNG was assumed to equal to 1 $m^3$ and a temperature of -162 °C. The effects of boundary conditions on the base case were analysed lately. Hence, the pool diameter was variated from 5.0 to 6.4 m, following the typical pool height suggested by the literature (Nguyen et al., 2017). The evaporation rate was variated within the range 0.071 to 0.195 kg $m^{-2}$ $s^{-1}$ to include the results provided either by ideal models or experimental campaigns. The main parameters affecting the dispersion of LNG vapours are related to the atmospheric condition, i.e., wind velocity, atmospheric stability, humidity, and the heat flux from the substrate (ground or water). In this work, an ambient temperature of 25 °C was considered. The atmospheric Pasquill classes D (neutral) were associated with a wind velocity equal to 5 m $s^{-1}$, and a relative humidity equal to 40% was implemented and assimilated to dry and sunny conditions. On the other hand, the atmospheric Pasquill class F (very stable), associated with a wind of 2 m $s^{-1}$, and a relative humidity equal to 70 %, was applied to represent wet and foggy climatic conditions. For all the simulations, the wind was considered orientated in the positive x-direction. Regarding the heat flux from the ground to the vapour, 313.5 W $m^{-2}$ (Coyote3), 38.8 W $m^{-2}$ (MaplinSand27), and adiabatic conditions were also tested.

*Table 1: Boundary conditions adopted for the base case scenario defined in this work.*

| Boundary condition | Value |
|---|---|
| Ambient temperature [°C] | 25 |
| Atmospheric stability class | D |
| Wind velocity [$ms^{-1}$] | 5 |
| Wind direction | Positive x-direction |
| Humidity ratio [%] | 40 |
| Initial LNG temperature [°C] | -162 |
| Initial LNG volume [$m^3$] | 1 |
| Pool diameter [m] | 5.4 |
| Pool depth [m] | 0.04 |
| Evaporation rate [$kgm^{-2}s^{-1}$] | 0.071 |
| Heat flux from the ground [$Wm^{-2}$] | 313.5 |

The effect of the presence of objects on the dispersion was consequently investigated on a simplified layout of a typical port facility. The presence of the jetty and a liquefied gas carrier docked were considered. The LNG pool was deemed to be formed between the ship and the jetty in correspondence with the gas carrier manifold.

The pool size on y-direction was equalized to the size of a typical fender and, the size on x-direction was derived by the pool depth and released volume. The geometrical features of the liquefied gas carrier were posed similar to JS Ineos Intrepid - IMO 9685449, resulting in an overall length equal to 180.3 m (x-direction), overall breadth of 26.6 m (z-direction) and, a total height of 20m (y-direction). Furthermore, the quayside height above water was set to 2.0 m. Except for the geometrical features, all boundary conditions matched those of the base case. The defined numerical domain was extended to accommodate the obstacles, resulting in a 300 m long (x-direction), 30 m height (y-direction), and 50 m wide (z-direction) domain. Temperature, methane mole fraction, and relative humidity were calculated as a function of time and space for all the reported scenarios. Therefore, the dispersion safety factor (DSF) was evaluated following Equation 1.

$$DSF = \frac{LFL_x}{VIS_x} \tag{1}$$

The $VIS_x$ was assumed as the maximum distance where the measured temperature was equal to the dew point ($T_{dew}$) for at least one second. The $T_{dew}$ was calculated by using Bosen's correlation (Bosen, 1958), reported below:

$$T_{dew} = \left(\frac{H}{100}\right)^{\frac{1}{8}} (112 + 0.9 \cdot T_a) + 0.1 \cdot T_a - 112 \tag{2}$$

where H is the relative humidity expressed in percentage and $T_a$ is the ambient temperature in Celsius, respectively. The effects of the input parameters variated in this work on the length of the flammable region and visible cloud on the downwind direction were expressed in terms of normalized sensitivity coefficients ($NSC_{LFL}$ and $NSC_{VIS}$, respectively), as defined in Eq 3):

$$NSC_{\varphi} = \frac{d\varphi/\varphi}{d\chi/\chi} \tag{3}$$

where φ represents the generic calculated variable (i.e., $LFL_x$ and $VIS_x$) and χ the generic input parameter (i.e., the evaporation rate, heat flux from the substrate, pool diameter, wind speed, and relative humidity). A schematic representation of the proposed procedure is shown in Figure 1.

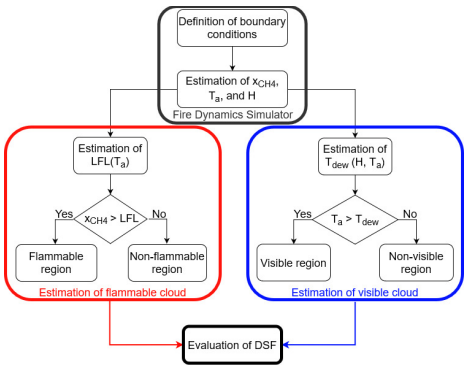


*Figure 1. Procedure for evaluating the sizes of the flammable (left, red box) and visible (right, blue box) clouds.*

## 3. Results and discussion

Considering the consumption of the liquid pool and the dispersion of the vapour cloud, the investigated scenario is intrinsically characterized by transient states. However, estimations were compared at the time, maximizing $LFL_x$ following a conservative approach. An increase in height reduces the size of the flammable region in the downwind direction. Indeed, the maximum $LFL_x$, equal to 35 m, was registered at 0.25 m above the sea level after 60 s from the pool formation. This value agrees with data reported by port authorities for bunkering operations of LNG (Port Authority of Gothenburg, 2017). Conversely, the application of the simplified graph suggested by the ISO 20519: 2017 to the present case will lead to $LFL_x$ equal to 65 m, indicating the over-conservativeness of this correlation. Noteworthy, a similar $LFL_x$ (i.e., 75 m) was obtained with the most conservative value of evaporation rate (i.e., 0.195 kg $m^{-2}$ $s^{-1}$), generally considered for large-scale scenarios, only (Luketa-Hanlin, 2006). Therefore, 0.25 m was considered to evaluate the length of the flammable region unless otherwise noted. On the other hand, similar cloud dimensions can be observed if lower concentrations (e.g., half LFL) are considered, suggesting that the cloud acts as a light gas when the methane volume fraction is smaller than 5 %v/v. Considering the relation between temperature and density, this implies that the temperature and composition of the cloud can be locally correlated, being determined by thermal and mass mixing, respectively. The dispersion safety factor DSF can be calculated by comparing the relative humidity at the dew point with the measured temperature. Hence, the combination of these distributions provides valuable

insights. Considering the state of matter and, thus, the density of the species involved in the investigated conditions, this comparison was reported in the proximity of the ground (Figure 2).

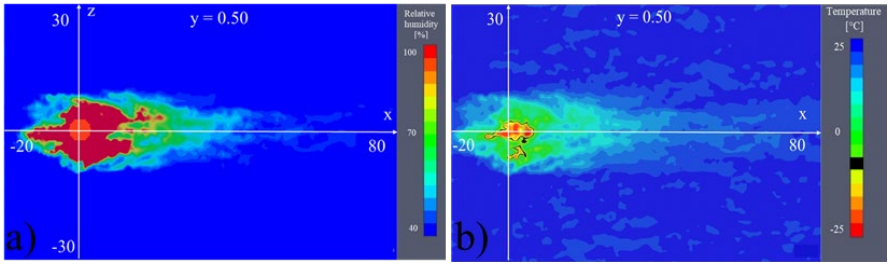


*Figure 2: Relative humidity (a) and temperature (b) distributions at 0.50 m above the sea for the Base case.*

Temperature below -10 °C can be registered only in correspondence to the liquid pool. Recalling that LFL of methane slightly variates in the range -10 °C – 30 °C (Pio and Salzano, 2019), the hypothesis of LFL is equal to 5 $\%_v$ for the determination of the flammable region can be considered as validated. Based on the observations reported before, LNG vapour mainly spreads horizontally, at first, because of the dense-gas behaviour at low temperatures. Then, by increasing the temperature, vapour behaves as light gas. Considering the significant impact of temperature on vapour density, the distance and time where this transition occurs are potentially affected by the thermal boundary conditions considered. Hence, the effect of the thermal boundary condition posed on the ground of the vapour cloud shape was evaluated at this stage. The reported data (Table 1) refers to scenarios where the thermal boundary condition on the ground was changed exclusively, whereas the other conditions were preserved as in the base case scenario. More specifically, Case 2 has q = 38.8 W $m^{-2}$, and Case 3 has q = 0.0 W $m^{-2}$. In this view, a cloud shape factor (CSF) was defined as the ratio between the maximum size of the flammable region on the horizontal axis (already adopted in this work and indicated as $LFL_x$) to the maximum size of the flammable region on the vertical axis ($LFL_y$).

*Table 1: The effect of thermal boundary conditions on flammable and visible regions.*

| Case | $LFL_X$ [m] | DSF [-] | CSF [-] |
|---|---|---|---|
| Base case | 35 | 1.23 | 16 |
| Case 2 | 110 | 1.10 | 220 |
| Case 3 | 130 | 0.72 | 230 |

As demonstrated by the CSF trend, reduced heat flux from the substrate promotes the vapour spreading on the horizontal axis. The hypothesis of adiabatic conditions results in a larger $LFL_x$, up to 3 times the value obtained for the base case. Besides, a similar value to the adiabatic case was observed once water properties were implemented. A comparison between $LFL_x$ and CSF shows that the base case is the only scenario where $LFL_y$ is larger than unity. The CSF trend for the imposed heat flux (q) can be satisfactorily represented ($R^2$ = 0.9997) by the following exponential correlation (Eq. 4) in the investigated range:

$$CSF = 120\, e^{-3q} \tag{4}$$

Conversely, the effect of this parameter on DSF is smaller. Besides, a monotonic trend cannot be observed because of the different impacts on $LFL_x$ and $VIS_x$.
Normalized sensitivity coefficients calculated in this work are reported in Figure 3.

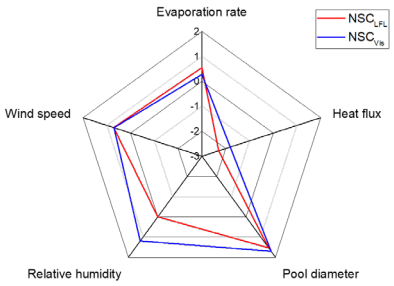


*Figure 3. Effects of input parameters on the length of the flammable region and visible cloud on the downwind direction expressed in terms of normalized sensitivity coefficients (NSC).*

The $NSC_{LFL}$ value for the evaporation rate approaches unity. This means that any error in the estimation of the evaporation rate propagates to the $LFL_x$ with almost the same relative amplitude, making the determination of this parameter essential. Similar considerations can be applied to the visibility concept, although reduced because of the smaller NSC. This aspect assumes significance if the uncertainties in the determination of the evaporation rate and the variability in experimental data collected for LNG are considered. Indeed, accurate models accounting for this property for cryogenic fuels are still under development/validation. Besides, several boundary conditions usually neglected in safety analyses (e.g., presence of waves and composition of the substrate material) may cause significant changes in the evaporation rate. The condition $NSC_{LFL} > NSC_{VIS} > 0$ implies that a more significant evaporation rate generates larger DSF, giving a different perspective to the comparison of the DSF estimated in this work for the base case scenario (i.e., 1.23) and the one reported in the literature [11] in similar conditions (i.e., 1.34). Indeed, in the latter case, a more conservative value for the evaporation rate was assumed. Either $LFL_x$ or $VIS_x$ shows large negative NSCs for heat flux, meaning that the thermal properties of the solid material that lays on the ground of surrounding areas should be included when LNG dispersion is modelled. This aspect is relevant for the LNG case, given the vapour density trend concerning the temperature. In other words, the heat transferred from the substrate to the vapour cloud plays a crucial role in determining the cloud temperature and, thus, the density distribution and the shape factor. Conversely, positive NSCs can be observed for pool diameter, indicating that the accurate characterization of the pool formation phase is essential for accurate characterization of the LNG dispersion scenario. Besides, the similarity in NSC values may mislead preliminary evaluations because of the limited effects on the DSF. Variation in relative humidity implies apparent alterations of the visible cloud size, whereas the extension of the flammable region is weakly affected by this parameter. Based on the reported results, it follows that wind velocity has similar effects on both monitored parameters, resulting in almost constant DSF, as reported by Vilchez et al. (2013). Considering that D and F's stability classes were coupled with a wind speed of 5 and 2 m $s^{-1}$, respectively, $NSC_{LFL} > 0$ implies that the atmospheric condition 5D represents the most conservative on the safe side for the investigated scenario.

The presence of obstacles (i.e., the LNG carrier ship and the dock) was analyzed for the base case scenario (Figure 4).

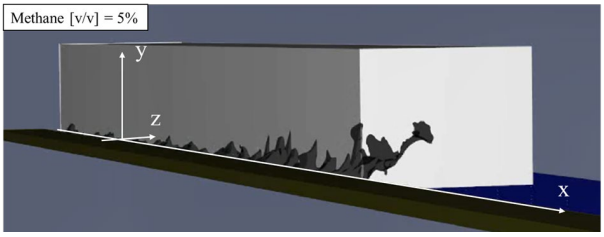


*Figure 4. Methane isosurface of concentration at the LFL for the base case scenario in the presence of obstacles.*

Quite obviously, the additional constraints represented by the ship's walls and dock considerably affect the shape of the flammable region. Indeed, the reduction in available space results in almost triple $LFL_x$ equal to 115 m, higher $LFL_y$ equal to 4 m, and a thinner cloud in terms of y-direction. A less stratified mixture can therefore be expected when obstacles are considered. As a matter of fact, without obstacles, at 0.5 m above the sea, the cloud is extended for 20 m on z-direction, while, in case of confinement, a large part of the cloud is localized between the harbour dock and the gas carrier. Once the confinement is removed, the immediate turbulence onset can be observed. This phenomenon increases the mixing efficiency and consequently reduces the nearby methane concentration. The increase in mixing efficiency affects thermal aspects, as well. Hence, the density of the vapour is lower, causing a larger $LFL_y$. A characteristic time ($t_d$) represents the flammable mixture's first appearance on the dock after the pool formation was defined. For the base case, a $t_d$ of 55 s was found. Following the procedure already implemented in the absence of obstacles, the extension of the visible cloud was estimated. In this case, $VIS_x$ equal to 64 m was found, resulting in a DSF of 1.80. Comparing the corresponding values for the base case scenario (i.e., $VIS_x$ = 28.5m and DSF = 1.23), it is possible to conclude that obstacles have a significant but diversified impact on the flammable and visible region. The latter can be ascribed to the formation of additional layers of cold vapours caused by the confinement and that alter the temperature distribution thus the size of the visible cloud.

## 4. Conclusions

This work shows the effects of input parameters on the dispersion of liquefied natural gas during the bunkering procedures. More specifically, the evaporation rate, the wind speed, the heat flux, the relative humidity of the atmosphere, and the liquid pool diameter were variated. The distribution of fuel concentration within the vapour cloud indicates that the flammable region calculated at 1 m above the sea level leads to unsafe estimations because of the elevated density of vapour in the first stage after the release. The lengths of the flammable and visible regions were determined for all the investigated conditions. The heat flux from the ground was found the most impacting parameter on the size of the flammable and visible areas, mainly because of the variation in the cloud shape. This result may be intended as an indication for the design of the dock area to promote dispersion in the desired direction. Then, a simplified layout representing a typical dock facility has been implemented. The presence of obstructions considerably increases the size of the flammable cloud along with the downwind direction. However, higher mixing efficiency was observed at the boundary between confined and unconfined areas, limiting the flammable area to the proximity of the ship. Eventually, the inclusion of obstacles generates a higher DSF ratio between the sizes of flammable and visible clouds, up to 50% higher than the corresponding conditions in an open environment. These aspects may assume an essential role in port area design and consequence analysis of LNG.

### References

Àgueda A., Subirana J., Pastor E., Schleder A. M., and Planas E., Revisiting the dispersion safety factor (DSF) for vapor clouds of liquefied flammable gases (LNG and propane), Saf. Sci., 128, 104748, 2020.

Blackmore D. R., Eyre J. A., and Summers G. G., Dispersion and combustion behavior of gas clouds resulting from large spillages of lng and lpg on to the sea, Trans. - Inst. Mar. Eng. TM, 1982.

Bosen J. F., An approximation formula to compute relative humidity from dry bulb and dew point temperatures, Mon. Weather Rev., 1958.

Chang Y. T. and Park H., The impact of vessel speed reduction on port accidents, Accid. Anal. Prev., 123, 422–432, 2019.

European Maritime Safety Agency, Guidance on LNG Bunkering to Port Authorities and Administration, 2017.

Fiates J., Santos R. R. C., Neto F. F., Francesconi A. Z., Simoes V., and Vianna S. S. V., An alternative CFD tool for gas dispersion modelling of heavy gas, J. Loss Prev. Process Ind., 44, 583–593, 2016.

Fy G., Wand J., and Yan M., "Anatomy of Tianjin Port Fire and Explosion: Process and Caused," Process Saf. Prog., 35, 2016.

ISO 20519: 2017, Ships and marine technology — Specification for bunkering of liquefied natural gas fuelled vessels, 2017.

ISO / TS 18683: 2015, Standards Publication Guidelines for systems and installations for supply of LNG as fuel to ships," 2015.

Luketa-Hanlin A., A review of large-scale LNG spills: Experiments and modeling, Journal of Hazardous Materials. 2006.

McGrattan K., Hostikka S., McDermott R., Floyd J., and Vanella M., Fire Dynamics Simulator User's Guide, NIST Spec. Publ. 1019 Sixth Ed., 347, 2019a.

McGrattan K., Hostikka S., McDermott R., Floyd J., Weinschenk C., and Overhold K., Fire dynamics simulator (FDS) validation technical reference guide volume 3: Validation, NIST Spec. Publ. 1018, 3, 2019b.

Nguyen L. D., Kim M., and Choi B., An experimental investigation of the evaporation of cryogenic-liquid-pool spreading on concrete ground, Appl. Therm. Eng., 123, 196–204, 2017.

Nigata Loading system LTD, Marine Loading Arms, 2019.

Osorio-Tejada J. L., Llera-Sastresa E., and Scarpellini S., Liquefied natural gas: Could it be a reliable option for road freight transport in the EU?, Renew. Sustain. Energy Rev., 71, 785–795, 2017.

Pio G., Carboni M., Iannaccone T., Cozzani V., and Salzano E., Numerical simulation of small-scale pool fires of LNG, J. Loss Prev. Process Ind., 61, 82–88, 2019.

Pio G. and Salzano E., The effect of ultra-low temperature on the flammability limits of a methane/air/diluent mixtures, J. Hazard. Mater., 362, 224–229, 2019.

Plasmans J., Donnat L., de Carvalho E., Debelle T., Marechal B., and Baillou F., Challenges with the use of CFD for major accident dispersion modeling, Process Saf. Prog., 32, 207–211, 2013.

Port Authority of Gothenburg, LNG Bunker Operation Regulations, 2017.

Rauchegger C., Bayley S., Schröder V., and Thévenin D., Dispersion of heavy gases – Experimental results and numerical simulations, Process Saf. Prog., 34, 280–285, 2015.

Smagorinsky J., General circulation experiments with the primitive equations, Mon. Weather Rev., 91, 99–164, 1963.

Vílchez J. A., Villafañe D., and Casal J., A dispersion safety factor for LNG vapor clouds, J. Hazard. Mater., 246–247, 181–188, 2013.